Solid State Ionics 326 (2018) 200–204

Contents lists available at ScienceDirect

Solid State Ionics

journal homepage: www.elsevier.com/locate/ssi

Effects of intergranular barrier fluctuations on the electrical conductivity of polycrystalline semiconductors

A.J. Uriz[a], C. Buono[b,*], C.M. Aldao[b]

[a] Institute of Electronics Science and Technology (ICYTE), University of Mar del Plata and National Research Council (CONICET), Juan B. Justo 4302, B7608FDQ Mar del Plata, Argentina

[b] Institute of Materials Science and Technology (INTEMA), University of Mar del Plata and National Research Council (CONICET), Juan B. Justo 4302, B7608FDQ Mar del Plata, Argentina

ARTICLE INFO

Keywords:
Polycrystals
Intergranular barriers
Bricklayer model
Electrical conduction

ABSTRACT

We studied the influence of intergranular barrier fluctuations on the electrical response of 3D semiconductor polycrystals. We first computed with a numerical simulation model the dispersion in the intergranular barrier height on polycrystalline tin oxide due to the punctual character of the donors. Then, in order to quantify the effects of the barrier fluctuation in the overall conductivity of the semiconductor, we added the dispersion to the well known brick-layer model and determined the connection between impedance measurements and grain boundary resistivity. We found that, the brick-layer model gives lower values for the real intergrain resistivity. However, the error can be quantified indicating that the brick-layer model is not a bad approximation to determine electrical properties of intergrains of a polycrystal, specially for relatively large grains.

1. Introduction

Since long ago, polycrystalline semiconductors have been of interests in many applications in which controlling the electrical properties of the material is crucial [1–6]. Therefore, mechanisms involved in the transport properties are of central interest. It is regularly accepted that, in many cases, the electrical conduction of polycrystalline semiconductors is dominated by inter-granular potential barriers that have a Schottky-type nature [7–16]. In particular, oxide semiconductors regularly present a dominant density of oxygen vacancies that confer an n-type character to the grains.

In analyzing experimental results, researches often use the bricklayer model, in which it is assumed that the microstructure can be described by a stacking of cubic-shaped grains of the same size and that intergranular interfaces present identical properties. Despite its limitations, the bricklayer model can be considered valid in cases having a relatively narrow distribution of grain size. Microstructure impact on the performance of composite materials has been addressed by several authors [17–20]. In Ref. [20], in particular, Dezanneau et al. used Voronoi polygons or polyhedra (for a 2D or a 3D model) of progressive disorder to build a resistor network that describes the electrical properties of the resulting microstructure. Specifically, they considered that every node represents a grain that is connected to other grains with resistances inversely proportional to the contact line or area (for a 2D or 3D models, respectively). Then, the electrical conductivity of the system is determined by solving the resulting resistor network.

In the present work, we focus on another source for intergranular resistance value fluctuations. It is customary to model the electrostatic potential in a Schottky barrier with a one-dimensional quadratic potential, as it is obtained from a jellium of charge in the depletion region. However, the punctual character and random nature of the impurity positions lead to inhomogeneities that can significantly affect the conductivity [21]. As a consequence, the resulting resistances due to the intergranular barriers can be different, even though grains are of the same size and they have the same contact area. We specifically studied the effect of inter-granular barrier fluctuations on the resistivity for a cubic network. With a computational numerical simulation model, we determine the spatial fluctuations of the barriers due to the discreteness of the donors and their statistical distribution at the depletion region in order to determine the intergrain conductivity. Then, the obtained resistivity distribution is used to build a resistor network and its resulting overall resistance is calculated for tin oxide.

2. Intergranular barriers fluctuations

The electrical properties of polycrystalline semiconductors are usually described with a simple one-dimensional model representing the interface between two grains, which dominates the overall

* Corresponding author.
E-mail address: cbuono@mdp.edu.ar (C. Buono).

https://doi.org/10.1016/j.ssi.2018.10.002
Received 13 July 2018; Received in revised form 3 September 2018; Accepted 4 October 2018

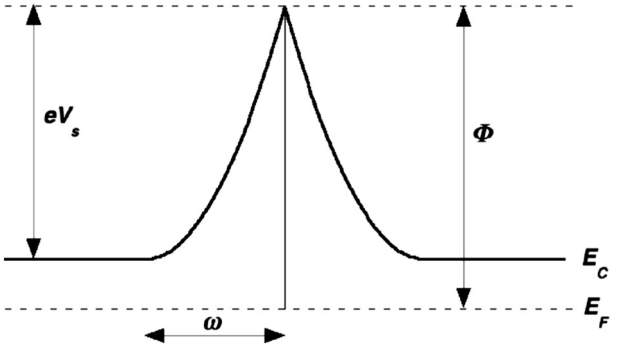

Fig. 1. Diagram for the intergranular double-Schottky barrier model. The band bending is eV_S, ϕ is the height of the barrier, and ω is the width of the depletion region. E_C is the bottom of the conduction band and E_F is the Fermi level.

conductivity. By solving Poisson's equation for the depletion approximation, the relationship between the band bending and the depletion region width ω is [7]

$$V_s = \frac{eN_d}{2\varepsilon_r \varepsilon_0}\omega^2, \tag{1}$$

where V_s is the band bending (in volts), N_d the doping, ε_0 the vacuum permittivity, and ε_r the relative permittivity.

Fig. 1 depicts the double Schottky barrier model that is generally accepted to describe an intergranular interface for an n-type semiconductor. The underlying assumption in this analysis is that the potential barrier has the same height and shape along the whole interface. In fact, this is an approximation because the potential barrier arises from the Coulomb potential due to all present charges and then fluctuations are unavoidable.

Following Mahan [22], we calculated the electrostatic potential due to a double Schottky barrier, arising from a random distribution of dopants in the depletion regions. We built a parallelepiped of size $x \times y \times z$ shown schematically in Fig. 2. The width of the parallelepiped z is 2ω, were ω is the depletion region width from Eq. (1). We randomly distribute a finite number of doubly-charged donors inside the parallelepiped in $-\omega \le z \le \omega$ except in the plane $z = 0$ that corresponds to the grain-boundary. Then, we associate to each doubly-charged donor two equal and opposite charges in the interface, at the grain-boundary; with this arrangement there is charge neutrality. For our simulations we chose an average band bending of 0.8 eV, a doping concentration $N_d = 5 \times 10^{23}\,\mathrm{m}^{-3}$, and a relative permittivity $\varepsilon_r = 12.3$, values that are commonly reported for tin oxide. Using Eq. (1), for these values, ω can be calculated to be 46.6 nm. More details can be found in Ref. [21].

The electrostatic potential in every point of the system was

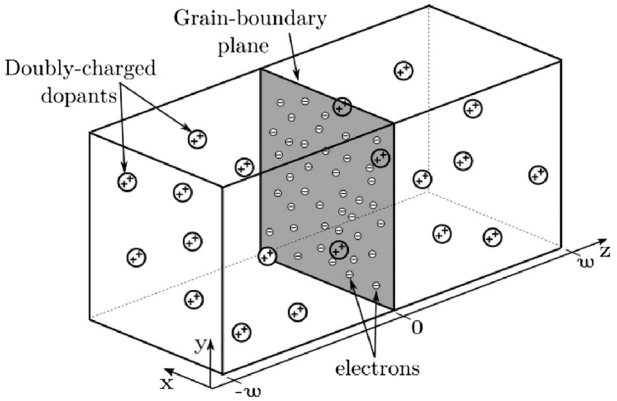

Fig. 2. Schematic diagram of the numerical simulation geometry and the arrangement of the punctual charges.

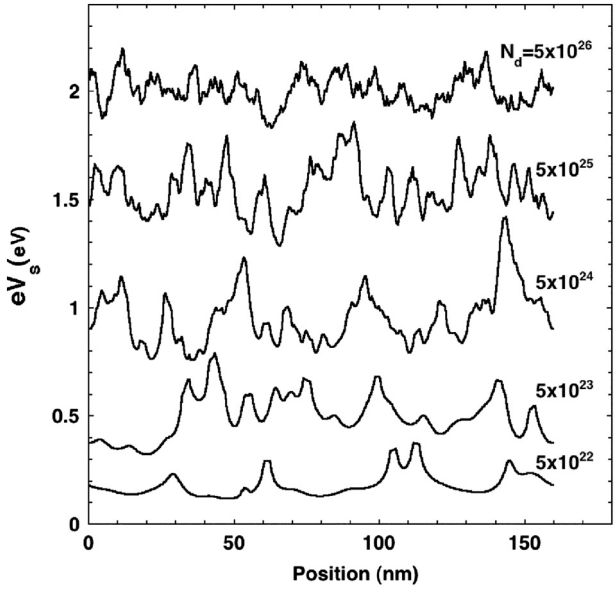

Fig. 3. A sample portion of the barrier height as a function of the position for a back-to-back Schottky barriers for different dopings. Dopants are doubly charged, and the average band bending is 0.8 eV. For clarity, curves were offset on the vertical axis.

computed as the sum of the Coulomb potentials generated by all charges. The band bending at the interface is defined as the maximum electrostatic potential in the direction normal to this plane (z direction) for every point in the parallelepiped. Periodic boundary conditions were used to avoid edge effects. We used doubly charged dopants, as oxygen vacancies doubly ionized in metal oxides and tin oxide in particular. Sample subsections of the barrier height for different dopant concentrations N_d as a function of position in the y direction for a fixed x is shown in Fig. 3.

Interestingly, fluctuations are not very dependent on doping. Also, in principle, it could be thought that fluctuations should decrease with N_d, as observed for the larger studied dopings. However, results indicate that, for low dopant concentrations, fluctuations increase with N_d. The reason for this unexpected result can be unveiled by looking the result for the lowest doping. Note that the lowest the doping, the larger the average distance between charges and then regions relatively flat appear. Eventually, for large dopant concentrations, charges responsible for band bending are very close, charge density is more homogeneous and then fluctuations decrease.

3. Intergranular effective resistance

Conduction in polycrystals has been interpreted in analogy to those in metal-semiconductor contact diodes. Accordingly, the electrical properties of polycrystalline semiconductors are usually described with a simple one-dimensional model representing the interface between two grains as shown in Fig. 1. We chose an n-type semiconductor because in tin oxide oxygen vacancies are the dominant defects and they behave as donors.

It is regularly considered that a thermionic mechanism is responsible for the sample conductivity. Thus, the transport mechanism corresponds to the emission of electrons over the top of the barrier and then the current density from one grain to a contiguous one is given by

$$J_{thermoionic} = A^* T^2 \exp(-\Phi/kT). \tag{2}$$

A^* is the Richardson constant that it has the value.

$$A^* = 4\pi m^* e k^2/h^3 \tag{3}$$

where m^* is the effective mass and h the Planck constant.

Like in metal-semiconductor junctions, electrons have other ways to be transported in a polycrystal. Indeed, electrons with energies below the top of the barrier can penetrate the barrier and reach the other grain. This is known as quantum-mechanical tunneling. The number of electrons decreases exponentially with energy and the barrier to tunnel becomes lower and thinner. Thus, many electrons cross the barrier at energies between E_C at the bulk and the top of the barrier.

The current density due to quantum-mechanical tunneling can be calculated summing up the contribution of all electrons arriving to the barrier,

$$J_{tunneling} = \frac{A^* T}{k} \int_0^{eV_s} F(E)P(E)dE, \tag{4}$$

where *F(E)* is the Fermi-Dirac distribution and *P(E)* is the transmission probability. *P(E)* can be calculated using the Wentzel-Kramers-Brillouin approximation as

$$P(E) = \exp\left[-2\int_a^b a(z)dz\right] \tag{5}$$

where a and b correspond to the values of z where E equals the electrostatic potential and α is given by

$$a = 2\pi\frac{\sqrt{2m(eV(z) - E)}}{h} \tag{6}$$

After integrating Eq. (5) for a parabolic barrier, *P(E)* is

$$P(E) = \exp\left\{-\frac{(eV_s)^{1/2}\omega\sqrt{2m}}{\hbar}\left[\left(1 - \frac{E}{eV_s}\right)^{1/2} - \frac{E}{eV_s}\ln\left(\frac{1 + \left(1 - \frac{E}{eV_s}\right)^{1/2}}{\left(\frac{E}{eV_s}\right)^{1/2}}\right)\right]\right\}, \tag{7}$$

where $h = h/2\pi$.

Now, Eq. (4) can be applied using any regular computing method.

A double Schottky barrier model is widely accepted to describe polycrystalline semiconductor intergrains. However, many researchers consider grain boundaries of essentially zero width, while others take into account a non-negligible disordered layer at the grain boundaries, such that the electron transport occurs in two steps [23]. Since the main conclusions of this work will not differ, for the sake of simplicity we adopted here the second assumption. Depending on the dopant concentration and temperature, the tunneling contribution can be the most relevant conduction mechanism in many cases. In the present case, both contributions are of similar magnitude.

With Eqs. (2) and (4), the thermionic and tunneling contributions to conduction can be figure out. These equations are valid for specific barriers. As discussed in Section 2, barriers fluctuate at the intergrain as shown in Fig. 3. Therefore, we need to integrate the contributions to conduction along the intergrain surface to determine the overall conductance. This means that the total current crossing an interface of area A is

$$I_{tot} = \frac{1}{A}\iint I(x,y)dxdy, \tag{8}$$

where A is the intergrain area and *I(x,y)* the current at (x,y) of the intergrain surface. The integral must be carried out over the intergrain area A. The effective resistance can be determined by applying a small voltage (say 0.001 V) and determining the current through the intergrain along the whole surface.

Barrier fluctuations depend on the specific donor distribution within depletion regions. Since donors are randomly distributed, barriers fluctuations are different for any specific intergrain and then the effective resistance does not have always the same value but it presents dispersion around a mean value. Fig. 4 shows the resulting histograms for intergrains of side $L = 40$ nm and 179 nm, normalized to the average resistance. As we can expect, the dispersion reduces with the intergrain size because barrier heights result from a random distribution of charges. The larger the grain, the larger the interface area, which is equivalent to have a larger sample implying smaller fluctuations.

We found that results of Fig. 4 can be very well fitted with a log-normal distribution, which is the statistical realization of the multiplicative product of many independent random variables. The log-normal distribution presents the following general form

$$f(x) = \frac{1}{\sigma\sqrt{2\pi}}\exp\left[-\frac{(1nx - u)^2}{2\sigma^2}\right] \tag{9}$$

In Fig. 5 we present the normalized resistance distributions with the intergrain size L as a parameter fitted with log-normal functions. Note that the distributions become narrower and more symmetric with the intergrain size.

4. Results and discussion

In order to test the influence of intergranular barrier fluctuations on the total conductivity of the polycrystal, we used the bricklayer model (BLM), which consists of a simple cubic resistor network, where the bonds between the nodes at the vertexes of the cubes are connected with resistances [24–27]. We incorporated to the BLM a dispersion to the resistances, with a log normal distribution as shown in Fig. 5. Each of the resistances in the resistor network represents the interface between the grains of the polycrystal.

First we build a cubic structure composed by a network of resistors of size $n \times n \times n$, then we assign to each resistor in the network a value of resistance taken from the log-normal distribution with parameters μ and σ given in Fig. 5. A scheme of the built structure is shown in Fig. 6. It can be seen that the nodes *N(i,j,k)* are the vertexes of each cube connected by resistances. These nodes are enumerated according of its position in the main cubic structure (see Fig. 6), which represents the grains bulk. The first index i is increased in the direction of the z axis of Fig. 2, *i.e.* the direction perpendicular to the intergrain.

Secondly, the cubic structure is excited using an ideal voltage generator of 1 V placed between the union of the nodes represented as *N(0,j,k)* and *N(n,j,k)*. Consequently, a DC current and equivalent resistance is obtained. We compute the resistance $R_{polycrystal}$ for different sizes of the resistor network $n = 3, 4, 5, 10, 20$ using the log-normal distribution parameters (μ and σ) as a function of the intergrain size L found previously (see Fig. 5). In order to take into the account the boundary conditions, resistors with the same statistical properties were included in the simulations between each pair of nodes *N(i,0,k)-N(i,n,k)*, and *N(i,j,0)-N(i,j,n)*. Also, to reduce statistical effects, which can bias the simulations, for each combination of L and n, 10 executions of the simulation were performed and results were averaged. Then, as a reference for each value combination of L and n, a cubic structure composed of equal resistors whose value is the mean of each log-normal distribution (R_{BLM}), was implemented.

Fig. 7 presents the resistance of polycrystals related to that of the BLM ($R_{polycrystal}/R_{BLM}$) as a function of intergrain size L, for different values of the resistor network n. We observe that $R_{polycrystal}/R_{BLM}$ has a quick but limited increase with L for all values of n. This behavior was expected, since as the grain size increases, not only the mean values of the resistance decrease, but also the resistance distributions become narrower and more symmetric (see Fig. 5), and therefore the dispersion in the resistance is reduced. Thus, as expected, the ratio $R_{polycristal}/R_{BLM}$ tends to 1 as the intergrain size increases due to the dispersion decrease. What is more, it is expected that and increasing in the dispersion of the values of the resistors, gives lowest values of $R_{polycristal}$, since the lower resistance dominates the value of the equivalent resistor.

We can also see from Fig. 7 that, for a fixed intergrain size, the relation $R_{polycrystal}/R_{BLM}$ changes for the different values of n, due to

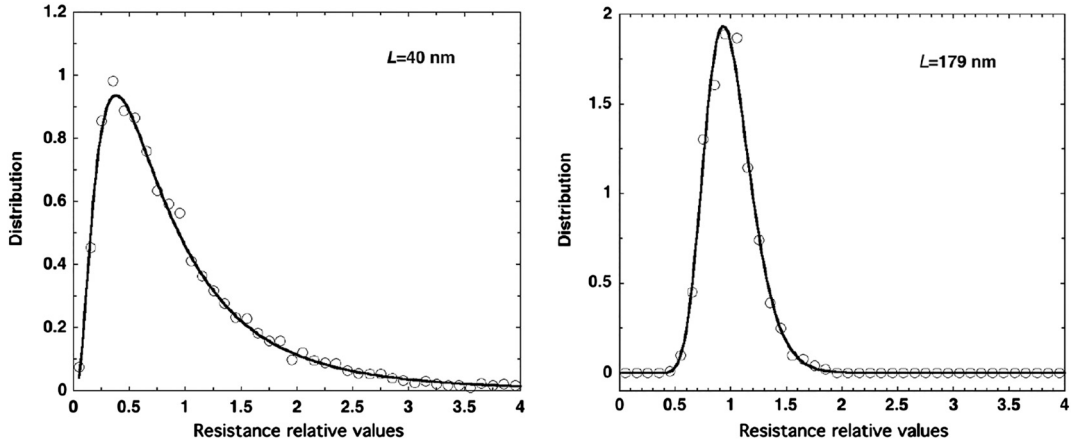

Fig. 4. Distributions of resistance values for two intergrain with sizes (a) L = 40 nm and (b) L = 179 nm. Numerical data (circles) were fitted with log-normal functions (lines).

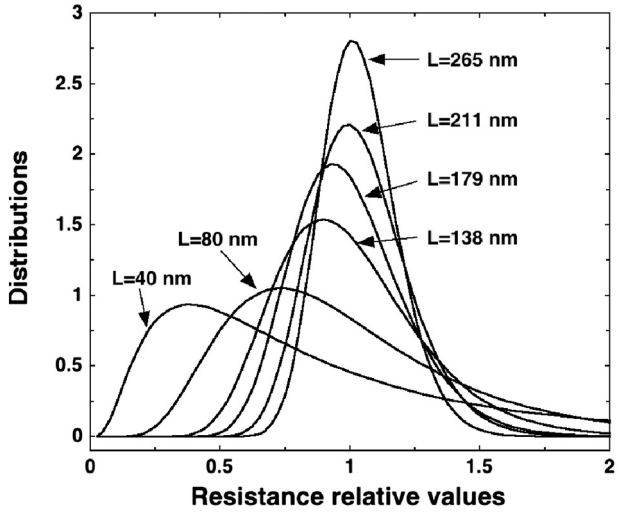

Fig. 5. Resistance values distributions for different intergrain sizes fitted with log-normal functions. Used values for (μ, σ) are: (−0.314, 0.807) for L = 40 nm, (−0.097, 0.465) for L = 80 nm, (−0.0349, 0.279) for L = 138 nm, (−0.0229, 0.216) for L = 179 nm, (−0.0237, 0.179) for L = 211 nm, and (−0.027, 0.1394) for L = 265 nm.

finite size effects. In the inset of Fig. 7, we plot, as an example, $R_{polycrystal}/R_{BLM}$ as a function of n, for a fixed intergrain size of 40 nm, and we can see that there is a significant variation for small n, but $R_{polycrystal}/R_{BLM}$ quickly converges to a fixed value, indicating that finite size effects are meaningful for sizes of the resistor network n bigger than 10.

In summary, we can see that differences for the brick-layer model with and without dispersion in the resistances ($R_{polycrystal}$ and R_{BLM} respectively) become relevant for very small intergrain sizes. With intergrain size the ratio $R_{polycrystal}/R_{BLM}$ converges to 1, indicating that, in order to obtain electrical properties, the brick-layer model without dispersion becomes a good approximation of a polycrystal structure for relatively large intergrains.

5. Conclusions

We have analyzed the effects of inter-granular barrier fluctuations on the electrical conductivity of polycrystalline tin oxide. Barrier fluctuations due to the discreteness of the donors and their statistical distribution at the depletion region of a back-to-back Schottky barrier were studied with a computational numerical model. We found that the barrier height fluctuations leads to a Log-Normal distribution for intergrain resistances that becomes narrower with the system size.

Then we proposed a modified brick-layer model, were the values of the resistances in the cubic structure are taken from the log-normal distribution found before, simulating an intergrain surface. We found that only for small intergrain sizes the brick-layer model with and without dispersion differ appreciably, indicating that the brick-layer model without considering the dispersion due to the fluctuations in the barrier height in the polycrystal, can be in many cases a good

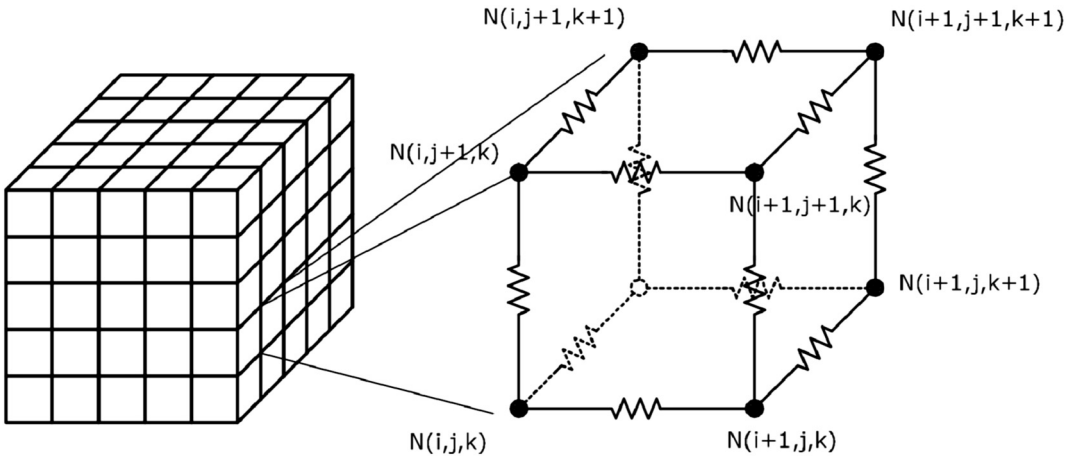

Fig. 6. Scheme of the resistor network with cubic structure. Each one of the cubes that form the main structure is composed of eight nodes linked by resistances.

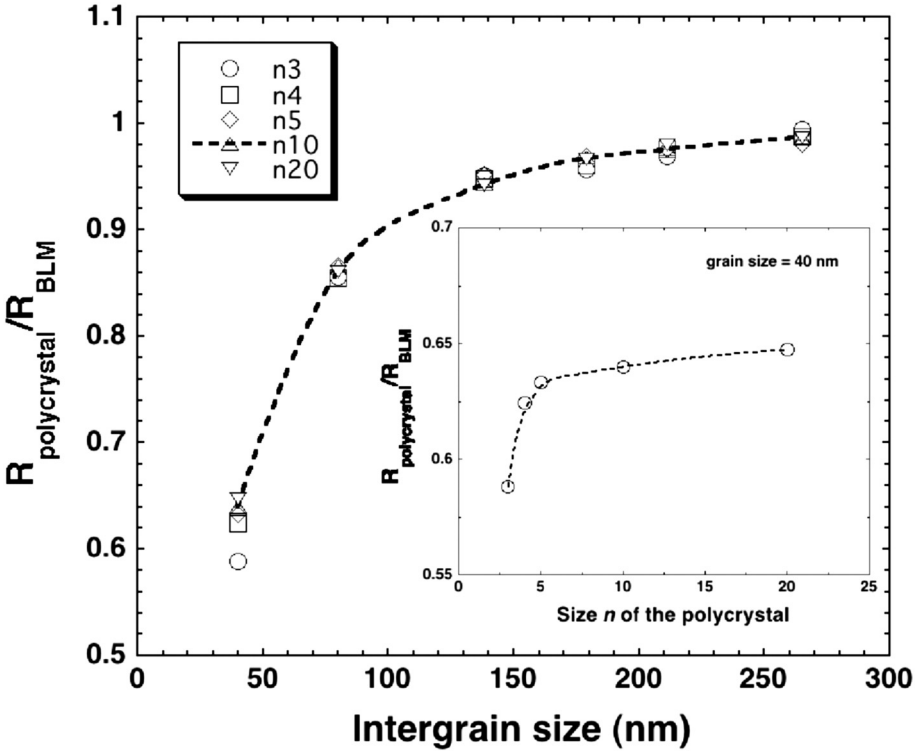

Fig. 7. Resistance of polycrystals related to that of the BLM as a function of intergrain size and cubes of different size n. Dashed curve is the fitting for $n = 10$. The inset shows the dependence on the polycrystal size for a intergrain size equal to 40 nm.

approximation to obtain electrical properties of a polycrystal intergrain.

Acknowledgements

This work was partially supported by the National Council for Scientific and Technical Research (CONICET) of Argentina and the National University of Mar del Plata (Argentina).

References

[1] H.J. Möller, H.P. Strunk, J. Werner, Polycrystalline Semiconductors, Springer, Erice, Italy, 1984.
[2] M. Radecka, P. Pasierb, K. Zakrzewska, M. Rekas, Transport properties of (Sn,Ti)O_2 polycrystalline ceramics and thin films, Solid State Ionics 119 (1999) 43–48.
[3] T. Kuratomi, K. Yamaguchi, M. Yamawaki, T. Bak, J. Nowotny, M. Rekas, C.C. Sorrell, Semiconducting properties of polycrystalline titanium dioxide, Solid State Ionics 154 (2002) 223–228.
[4] J.D. Major, Grain boundaries in CdTe thin film solar cells: a review, Semicond. Sci. Technol. 31 (2016) 093001.
[5] G. Han, S. Zhang, P.P. Boix, L.H. Wong, L. Sun, S.-Y. Lien, Towards high efficiency thin film solar cells, Prog. Mater. Sci. 87 (2017) 246–291.
[6] A. Mallick, D. Basak, Revisiting the electrical and optical transmission properties of co-doped ZnO thin films as n-type TCOs, Prog. Mater. Sci. 96 (2018) 86–110.
[7] M.J. Madou, R. Morrison, Chemical Sensing with Solid State Devices, Academic, San Diego, 1989.
[8] G.D. Mahan, L.M. Levinson, H.R. Phillipp, Theory of conduction in ZnO varistors, J. Appl. Phys. 50 (1979) 2799–2812.
[9] G.E. Pike, Semiconductor grain-boundary admittance: theory, Phys. Rev. B 30 (1984) 795–802.
[10] G. Blatter, F. Greuter, Carrier transport through grain boundaries in semiconductors, Phys. Rev. B 33 (1986) 3952–3966.
[11] N. Barsan, U. Weimar, Understanding the fundamental principles of metal oxide based gas sensors; the example of CO sensing with SnO_2 sensors in the presence of humidity, J. Phys. Condens. Matter 15 (2003) R813–R839.
[12] N. Yamazoe, Toward innovations of gas sensor technology, Sensors Actuators B Chem. 108 (2005) 2–14.
[13] M. Batzill, U. Diebold, The surface and materials science of tin oxide, Prog. Surf. Sci. 79 (2005) 47–154.
[14] J.J. Velasco-Vélez, U. Kunze, T. Hass, T. Doll, Co-adsorption processes, kinetics and quantum mechanical modelling of nanofilm semiconductor gas sensors, Phys. Status Solidi A 207 (2010) 924–929.
[15] Christian Kjølseth, Harald Fjeld, Øystein Prytz, Paul Inge Dahl, Claude Estournès, Reidar Haugsrud, Truls Norby, Space–charge theory applied to the grain boundary impedance of proton conducting $BaZr_{0.9}Y_{0.1}O_3-\delta$, Solid State Ionics 181 (2010) 268–275.
[16] D.R. Leitr, M. Cilense, M.O. Orlandi, P.R. Bueno, E. Longo, J.A. Varela, Phys. Status Solidi A 207 (2010) 457–461.
[17] J.C.C. Abrantes, J.A. Labrincha, J.R. Frade, Applicability of the brick layer model to describe the grain boundary properties of strontium titanate ceramics, J. Eur. Ceram. Soc. 20 (2000) 1603–1609.
[18] N.J. Kidner, N.H. Perry, T.O. Mason, The brick layer model revisited: introducing the nano-grain composite model, J. Am. Ceram. Soc. 91 (2008) 1733–1746.
[19] J. Fleig, J. Maier, The impedance of ceramics with highly resistive grain boundaries: validity and limits of the brick layer model, J. Eur. Ceram. Soc. 19 (1999) 693–696.
[20] G. Dezanneau, A. Morata, A. Tarancón, F. Peiró, J.R. Morante, Effect of grain size distribution on the grain boundary electrical response of 2D and 3D polycrystals, Solid State Ionics 177 (2006) 3117–3121.
[21] C. Buono, F. Schipani, M.A. Ponce, C.M. Aldao, Intergranular barrier height fluctuations in polycrystalline semiconductors, Phys. Status Solidi C 14 (2017) 1700069.
[22] G.D. Mahan, Fluctuations in Schottky barrier heights, J. Appl. Phys. 55 (1984) 980–983.
[23] M.S. Castro, C.M. Aldao, Appl. Phys. Lett. 63 (1993) 1077–1079.
[24] J.R. Macdonald, Impedance Spectroscopy, John Wiley & Sons, New York, 1987.
[25] X. Guo, R. Waser, Electrical properties of the grain boundaries of oxygen ion conductors: acceptor-doped zirconia and ceria, Prog. Mater. Sci. 51 (2006) 151–210.
[26] J.C.C. Abrantes, J.A. Labrincha, J.R. Frade, Impedance spectroscopy study of niobium-doped strontium titanate ceramics, J. Am. Ceram. Soc. 85 (2002) 2745–2752.
[27] E. Chinarro, J.R. Jurado, F.M. Figueiredo, J.R. Frade, Bulk and grain boundary conductivity of $Ca_{0.97}Ti_{1-x}Fe_xO_{3-\delta}$ materials, Solid State Ionics 160 (2003) 161–168.